# DEVELOPING PROTEIN TAGS FOR SECONDARY ION MASS SPECTROMETRY TO DETERMINE PROTEIN INTERACTION

An Undergraduate Research Scholars Thesis

by

MENA M. KOZMAN

Submitted to the Undergraduate Research Scholars program at
Texas A&M University
in partial fulfillment of the requirements for the designation as an

UNDERGRADUATE RESEARCH SCHOLAR

Approved by Research Advisors: Dr. Emile A. Schweikert
Dr. Michael J. Eller

May 2019

Major: Biology

# TABLE OF CONTENTS

# ABSTRACT

Developing Protein Tags for Secondary Ion Mass Spectrometry to Determine Protein Interaction

Mena M. Kozman
Department of Biology
Texas A&M University

Research Advisor: Dr. Emile A. Schweikert
Department of Chemistry
Texas A&M University

Research Advisor: Dr. Michael J. Eller
Department of Chemistry
Texas A&M University

The development of protein tags that enable the analysis of proteins with high multiplexity, in the context of cellular interactions. Nanoparticle and metal chelated tags were developed and utilized by Secondary Ion Mass Spectrometry (SIMS) for the detection and analysis of cell surface proteins. Small (5 nm in diameter) nanoparticles in addition to metal chelates were optimized for antibody conjugation and protein tagging. These tags feature unique metal signatures for easy detection and characterization using mass spectrometry. The tags were tested and characterized using massive cluster SIMS with event-by-event bombardment and detection and a time of flight (ToF) mass analyzer.

# ACKNOWLEDGEMENTS

I would like to thank my project instructor, Dr. Schweikert, as well as, Dr. Eller, and Dr. Verkhoturov, for their guidance and support throughout this project.

Thanks also go to my friends and colleagues at the Center for Chemical Characterization and Analysis for all their effort and time. I also want to extend my gratitude to the National Institute of Health and the National Science Foundation for their funding of this project.

# NOMENCLATURE

| | |
|---|---|
| SIMS | Secondary Ion Mass Spectrometry |
| nm | Nanometer |
| ToF | Time of Flight |
| MCP | Microchannel Plate |
| SAMPI | Surface Analysis and Mapping of Projectile Impacts |
| MTEGME | 1-Mercapto-(triethylene glycol) methyl ether |
| AuNPs | Gold Nano-Particles |
| MUA | 11-Mercaptoundecanoic Acid |
| UV-VIS | Ultraviolet–visible |
| BHHCT | 4,4″-Bis(4,4,5,5,6,6,6-heptafluoro-1,3-dioxohexyl)-o-terphenyl-4′-sulfony chloride |

# CHAPTER I

# INTRODUCTION

Protein expression on cell surfaces is significant for cell to cell communication. Analyzing the protein composition on the cell surface can also lead to the assessment of the current biological state of the cell. The ability to analyze such proteins can expand our knowledge of how cells communicate, and study how their communication may be influenced by experimental factors. This type of analysis can be applied to immunology, stem cell research, and cancer cell research. [1, 2, 3, 4] However, our goal is to analyze cell interaction within individual cells. More specifically, during the formation of a synapse between an Antigen Presenting Cell and a T Cell during an immune response. This interaction involves numerous proteins on either side of the synapse, forming on the cell surface. For the best understanding of how such cells communicate, as many proteins as possible must be analyzed simultaneously. However, additional information is also required to fully comprehend this interaction. In addition to the ability of tagging and quantifying as many proteins as possible, one must also be able to observe the surrounding microenvironment. In summary, one must be able to analyze proteins as well as the adjacent proteins to infer interaction at the nanoscale.

## Conventional Technique

Protein analysis is widely used in many fields and can be used to understand cell behavior and the underlying mechanisms of cellular functions. The most common method of protein analysis today, is immunofluorescence. Previous work showed that it is possible to map and localize proteins at the nanoscale using immunofluorescence, but it is limited in the number of tags it has to offer simultaneously. Attempting to analyze a complex surface that contains

many proteins shows how difficult and laborious this method would be. Since one can only tag a handful of proteins at a time, the experiment would have to be repeated several times followed by a compilation of the results from successive runs to put a comprehensive picture of the proteins encountered at the synapse together. As a result, fluorescent tags were replaced with metallic labels which can be identified by mass spectrometry. This approach, termed Mass Cytometry, is currently the method of choice for protein analysis.

**Mass Cytometry**

As noted, Mass Cytometry, uses a like fluorescent microscopy tagged antibodies to analyze proteins. The metal tags used in Mass Cytometry can be detected by mass spectrometry. A key advantage is the number of tags that can be analyzed simultaneously, is roughly 40, while immunofluorescence can handle a maximum of 12 tags. [1, 2, 5] However, one limitation of common mass cytometry techniques, is that they do not provide the context of the microenvironment surrounding the proteins. In other words, localization with neighboring cells is lost in the sampling process. This is because the technique requires the cells to be extracted from their tissue sample in order to be analyzed. However, information about the microenvironment surrounding the proteins is necessary to provide context for the proteins analyzed. The significance of analyzing proteins in their original microenvironment is to allow for inference of colocalization.

What makes metal tags distinguishable, is their unique mass and thus they must be analyzed used a mass spectrometer. This causes the analysis process to become more challenging than immunofluorescence, since experiments are performed under vacuum. Mass spectrometers are able to separate charged species based on their mass to charge ratio, thus the metal tags bound to the proteins must be desorbed from the surface and ionized. Two methods of molecular

desorption and ionization utilize a laser or an ion beam. Utilizing either one to determine protein colocalization requires event by event detection. Here, the desorption/ionization process occur, as separate events, coupled with separate collection of date from each event. Thus, if two separate metal tags are detected in a single event, they must originate from colocalized proteins within the impact volume. One aspect to consider is the probing area from which ions are emitted upon impact. The probing area must be large enough to, not only capture the tagged protein, but also detect any nearby tagged proteins that are present on the surface. This ability to detect two sperate tags that are bound to two different proteins in a single event is essential to assess the colocalization of those proteins within the probing area. This is why the utilization of lasers or ion beams vary significantly. Lasers are limited in their ability to be focused due to diffraction, thus they have a large desorption area. This limits the laser's ability to provide resolution beyond the microscale. Ion beams on the other hand, allow for single atomic or cluster projectiles to impact the surface one at a time. This means that emission of ions is local to the site of impact of the primary ion projectile, which is significantly smaller than the emission area due to a laser. This allows for resolution beyond the microscale and down to the nanoscale. Atomic ions are not suitable projectiles as the volume perturbed is too small to cause emission from two separate tags in a single impact. In order to increase emission of secondary ions, large clusters have been developed that enable two or more tags to be emitted in a single impact. Thus, the answer relies in an analytical technique that can both utilize metal tags and determine colocalization at the nanoscale.

**Secondary Ion Mass Spectrometry**

One technique that can fulfill both requirements is cluster Secondary Ion Mass Spectrometry (SIMS). This technique uses a primary source of cluster ions that can be

accelerated to impact a sample surface that results in the ejection of secondary ions. These ions are then mass analyzed, usually with a time of flight mass analyzer. SIMS instruments have already been used to analyze the chemical composition of micropatterned surfaces as well as cells. [6, 7, 8] SIMS have also been demonstrated to use isotopically enriched metal tags, for the detection of proteins, offering up to 100 tags measured simultaneously. [9] In addition, SIMS has been demonstrated to measure isotopically enriched biological samples including Drosophila with high-resolution quantification of the isotopes. [10] Furthermore, the Fletcher group have demonstrated SIMS to be effective in imaging biological samples and mapping small chemical compounds existing in cells such as lipids. [11,12,13,14] Additionally, the Ewing group utilized SIMS to image freeze-fractured cells. [15,16] They also developed a device that can test the lateral resolution for SIMS instruments. [17] In SIMS, different projectiles can be utilized to bombard a sample surface and cause desorption and ejection of secondary ions. One common projectile is $C_{60}^+$, this carbon cluster is ideal in its ability to be formed due to the stability of the final structure. This projectile has been used in subcellular chemical imaging of antibiotics in single bacteria. [18] Other common projectiles include gas clusters such as $Ar_n^+$ (n= 1-6,000) and $(CO_2)_n^+$ (n > 10,000) were used in SIMS imaging by the Winograd group. [19,20] Lastly, his group has also evaluated other projectiles. [21]

Thus, using large cluster nano-projectiles, and event-by-event analysis, single impact cluster SIMS will be a well suited method of combing the high sensitivity of immunofluorescence and the multiplexing capabilities of mass cytometry. In order for this to be accomplished, metal tags must be developed to be suitable for SIMS. First, they must be able to conjugate to antibodies and secondly, they must contain a unique metal signature that can be

detected and characterized. Thus, the outcome of this project will be to apply nanoparticle tags and metal chelates for the analysis of proteins, without extraction from their environment.

# CHAPTER II

# METHODS

## Instrumentation

The instrument for which the tags are developed for, is a custom build SIMS instrument at Texas A&M University. The experiments performed in the instrument are approximately under a 1 X $10^{-6}$ Torr vacuum. This instrument uses a liquid metal ion source, which generates a range of gold projectiles accelerated by a 20 kV potential shown in Figure 1, labeled "A". The source provides a continuous stream of gold particles that creates a beam. This beam is then focused using Einzel lens shown in Figure 1, Labeled "B". Additionally, a 250-micrometer aperture is used to collimate the beam and control the bombardment area. Using a Wien filter, labeled "C", specific gold clusters are selected for and filtered out as projectiles to impact the target. The two projectiles used in this study are $Au_{400}^{4+}$ and $Au_{2800}^{8+}$; they are utilized differently, depending on the purpose and nature of the experiment. At this point, these projectiles are then accelerated further with an additional 100 kV potential, shown in Figure 1. The beam of gold projectiles is then pulsed into single projectiles at a rate of 1,000 particles per second that bombard the target one at a time, as shown in Figure 1, labeled "I". It allows single impacts to be analyzed separately, which is a required parameter for the determination of colocalization of proteins.

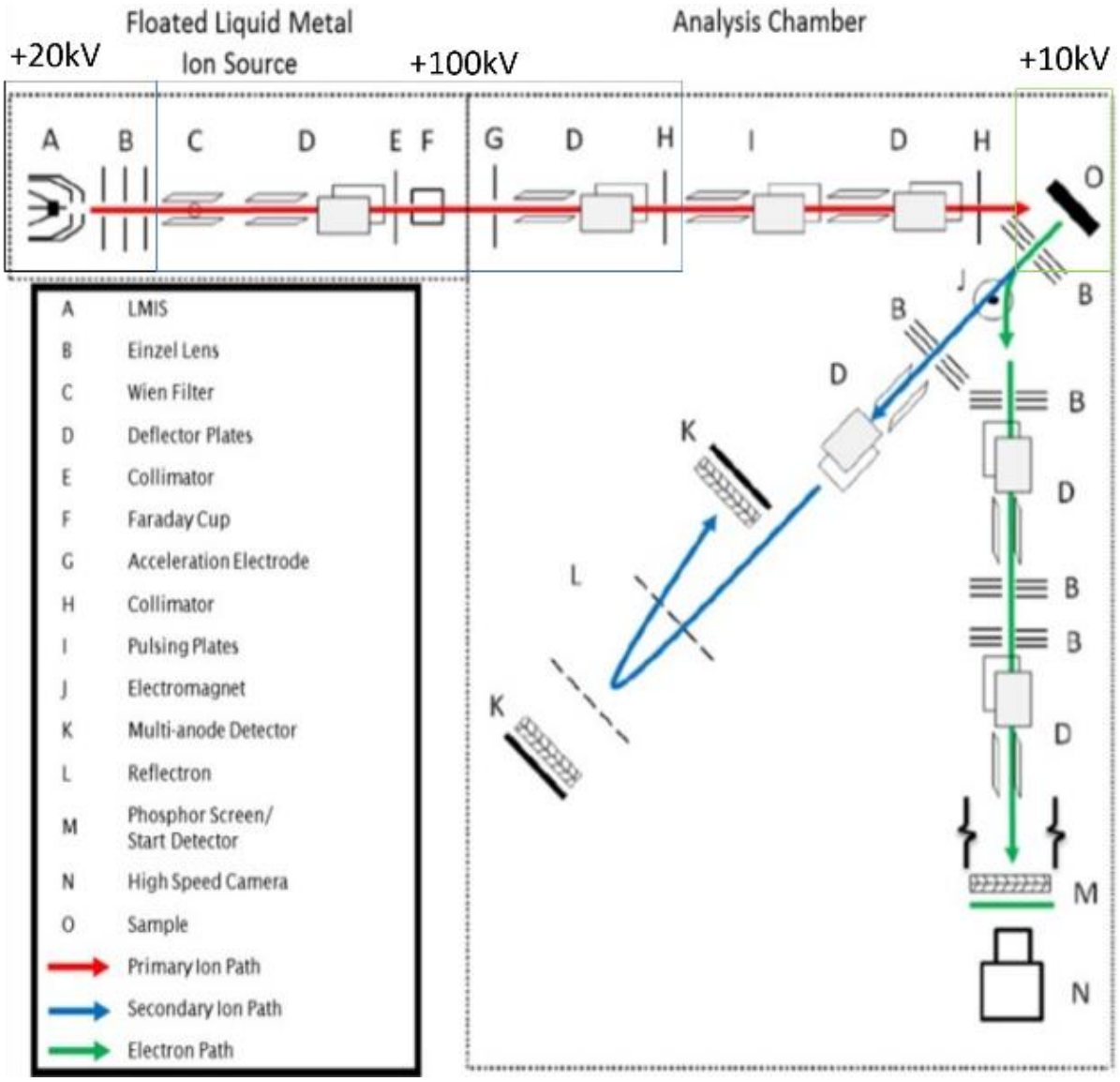


Figure 1. A schematic of the SIMS instrument. [22]

Upon the bombardment of the gold projectiles on the sample, electrons, ions, and neutrals are emitted from the surface. Initially, samples are deposited on a conductive plate of silicon. An electrical potential of -10 kV is then applied to the sample for rapid ejection of any negatively charged species including electrons. Thus, only negative ions are mass analyzed using a reflectron Time-of-Flight (ToF) mass analyzer. The reflectron ToF uses a weak magnetic field that deviates electrons to a start detector. This magnetic field is weak enough so that it does not cause significant deviation to the charged ions yet acts strongly on the light electrons. Since

electrons are tremendously lighter than a single atom, they are easily diverted away after the impact and are directed towards an electron detector. This starts a timer that measures the time for charged species to travel through a known distance. Since all emitted ions are accelerated using a constant potential, their speed becomes a function of their mass, with heavier ions being slower. Thus, the time it takes for a given ion to travel a known distance corresponds to its mass, in other words, heavier ions will take longer to travel the same distance than a lighter ion.

Detection of these ions is done through a Microchannel Plate (MCP) based 8-anode detector. The data is collected on an event-by-event fashion. This means that data is collected from each projectile separately, one impact causes the emission of secondary ions which are then collected and analyzed before the second impact occurs. This analytical feature is critical for the determination of colocalization between proteins. Data from these impacts is then processed and analyzed using a custom designed software called "Surface Analysis and Mapping of Projectile Impacts" (SAMPI). [23]

**Data Processing**

The first step in the processing of the data involves mass scaling the mass spectrum. This process combines the known exact mass of four species, and the time of arrival at each anode to calibrate and scale the entire spectrum, converting time measurements into a mass to charge unit. The total yield of any observed species can be obtained by summing the total count of the detected ion ($I_a$) and dividing it by the total number of impacts (N), as shown in Eq. 1.

$$Y_a = \frac{I_a}{N} \qquad \text{Eq. 1}$$

However, to determine colocalized species, coincidental yield must also be calculated. Since data is collected in an event-by-event fashion, individual mass spectra from certain impacts can be singled out and analyzed separately, this is necessary in calculating coincidental yield. For

example, to determine the coincidental yield of ion “A” with ion “B”, one must first single out all events that contain ion “B”. In other words, only events from which ion “B” was emitted and detected will be counted. That number of impacts will be called N(b). The next step is to calculate the total count of ion “A” in the subset of the spectra that were previously singled out containing ion “B”. By dividing that total $I_a(b)$ by N(b), the coincidental yield ($Y_{a,b}$) can be calculated. The coincidental yield equation is shown as Eq. 2.

$$Y_{a,b} = \frac{I_a(b)}{N(b)} \qquad \text{Eq. 2}$$

By taking the ratio of the coincidental yield over total yield, we get equation Eq. 3. By dividing the coincidental yield of ion “A” with ion “B” by the total yield of ion “A” we get a correlation coefficient donated as “C”. This correlation coefficient is greater than one when ion “A” is emitted more frequently with ion “B” than its normal emission frequency. If ion “A” is completely unrelated to ion “B”, then the frequency at which ion “A” is emitted with ion “B” would be the same frequency that ion “A” is emitted in general. This would result in a correlation coefficient close to one. Lastly, if ion “A” exhibits segregation away from ion “B”, then its emission with ion “B” is significantly less than its normal emission rate. In this case, the correlation coefficient would be less than one. This technique of analyzing correlation coefficients was utilized in signal characterization and peak assignment.

$$C = \frac{Y_{a,b}}{Y_a} \qquad \text{Eq. 3}$$

**Sample Preparation**

All samples were drop casted on a 10 mm x 10 mm silicon wafer. The wafers were cleaned and prepared by a series of sonication and washing with toluene, then acetone, followed by one more round of toluene, and lastly with water. The first sample was 10-micro liter deposit of a 20 mg/ml solution of 1-Mercapto-(triethylene glycol) methyl ether (MTEGME)

functionalized 5 nm gold nanoparticles (AuNPs) in toluene. Additional samples of MTEGME functionalized 5 nm AuNPs were resuspended and drop casted in water instead. This was accomplished by allowing the toluene solvent to evaporate away from a known amount of AuNPs. This known amount was then resuspended in various amount of water and the concentration was recalculated accordingly. Drop casting the nanoparticles in water solvent and allowing the water to evaporate in normal atmosphere proposed a challenge. Much of the analyte was deposited in a ring like formation instead of a thin even coating on the silicon wafer. This was problematic for SIMS analysis. Thus, the samples were then drop casted in ethanol atmosphere rather than regular atmosphere. The ethanol atmosphere would mix into the water droplet on the silicon wafer and weaken the surface tension, allowing the droplet to thin out on the wafer. This proved to be an efficient way of drop casting this sample. Several amounts of ethanol were tested to find the right amount of surface area exposure of ethanol that evaporated into the atmosphere. Six different amounts of ethanol exposure were tested, and the results can be seen below in Figure 2.

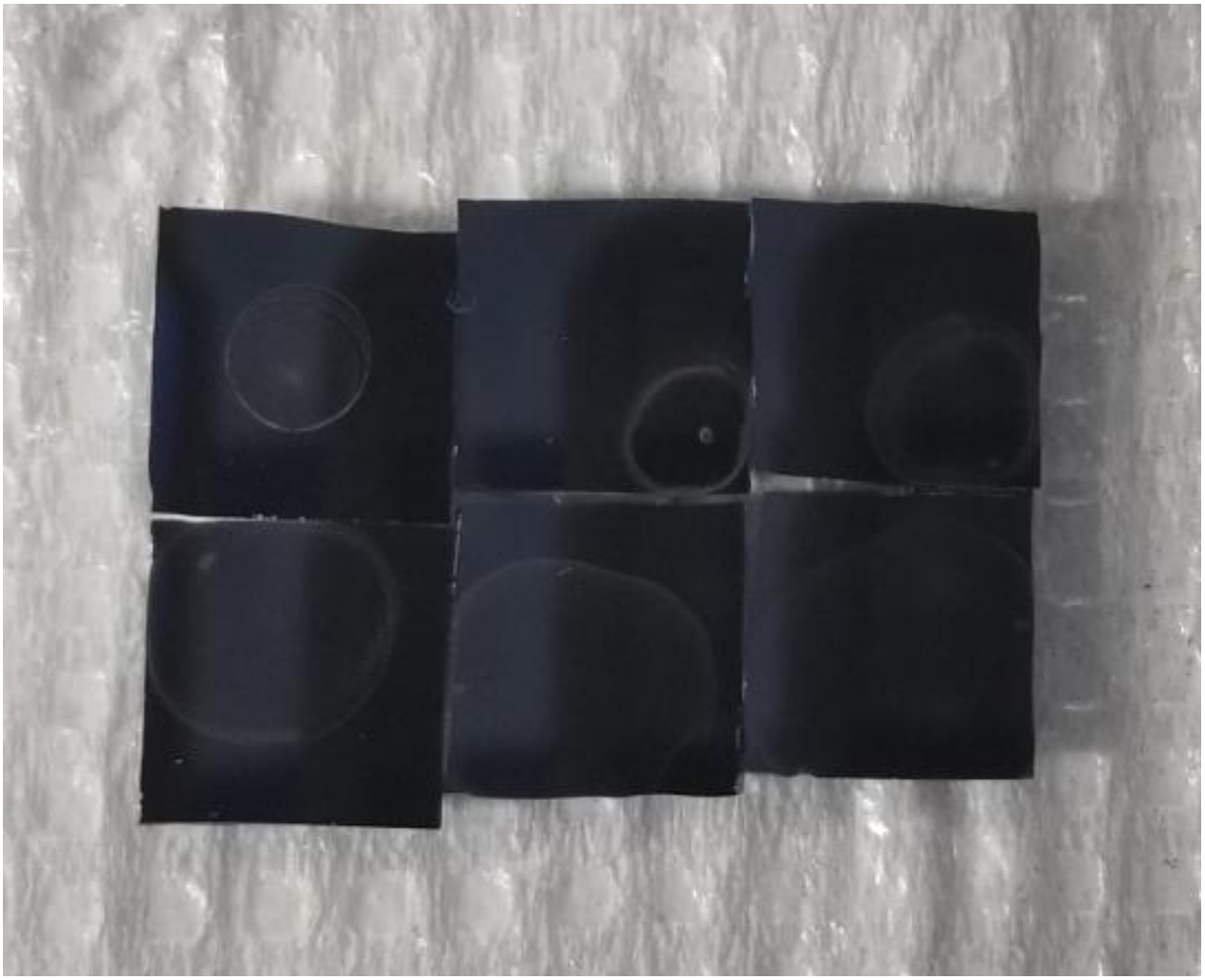

Figure 2. Drop cast results of increasing ethanol exposure from top left (least exposure) to bottom right (most exposure).

As seen above in figure 2, the top left sample was deposited under normal atmosphere, without the introduction of ethanol. The sample has clear bold concentric rings that contain most of the analyte, this leaves a very small number of nanoparticles in the middle to be analyzed by the mass spectrometer. However, as significant amount of ethanol is introduced into the atmosphere, it allows the analyte to deposited onto the wafer more evenly in a single a layer fashion rather than rings. When comparing the six wafers above, one could see how the sample appears to “fade” in with the wafer, which is indicative of an even distribution of the

nanoparticles along the surface. A schematic of the ethanol atmosphere apparatus was diagramed below in figure 3, for the bottom right sample which showed the best results.

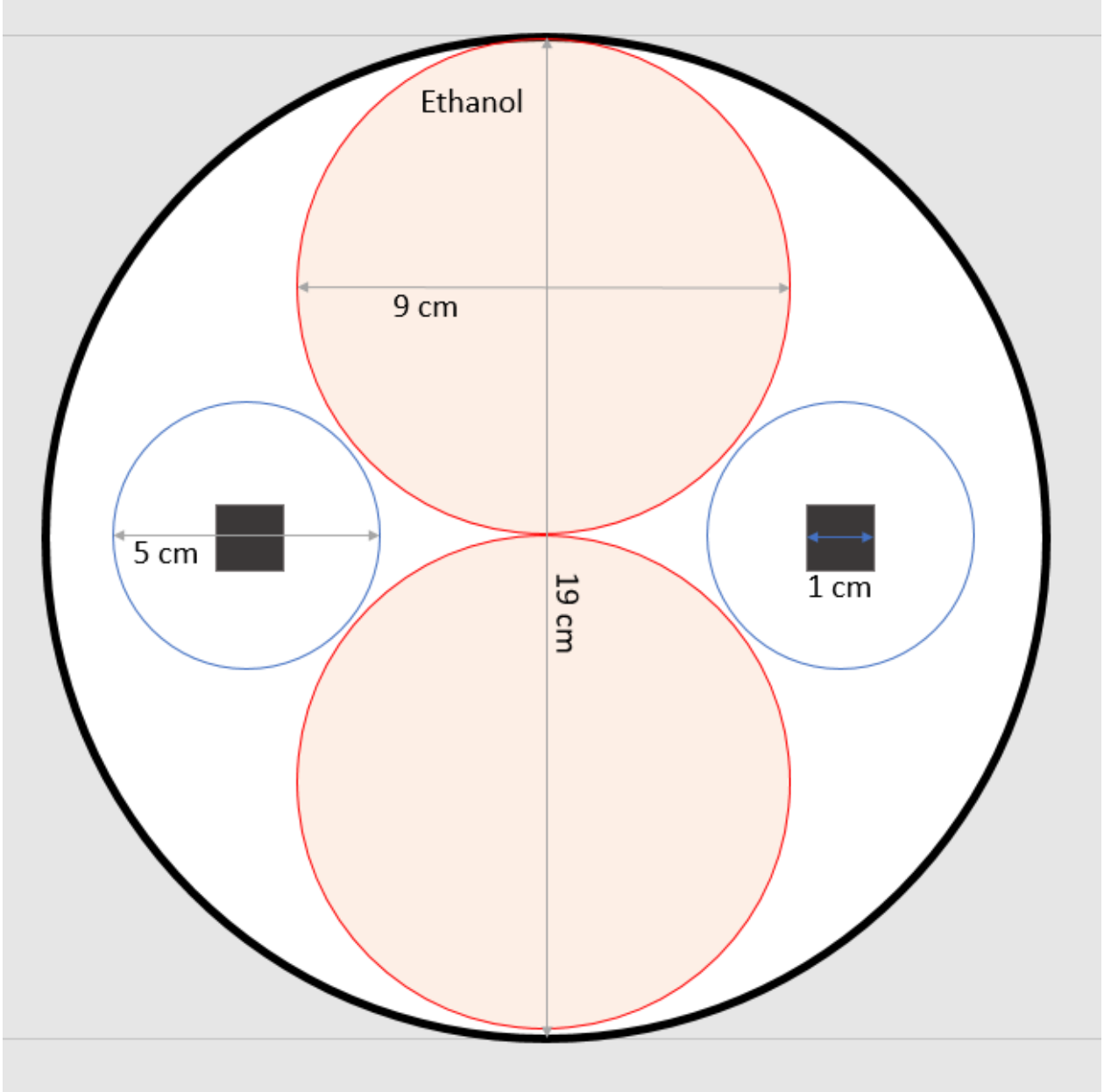


Figure 3. A schematic of the Ethanol atmosphere apparatus. Red/Orange represents ethanol, and the charcoal squares represent the silicon wafers.

The nanoparticles are originally functionalized with MTEGME, this ligand is not able to conjugate to antibodies. However, a ligand exchange reaction with 11-mercaptoundecanoic acid (MUA) is allowed to take place and is then stopped at different times. The reason for using MUA

is because it has a terminal carboxylic acid group which can be conjugated to antibodies. This reaction is carried out in toluene and the nanoparticles were centrifuged out at 3400 rpm for 1 hour at varied times. The centrifuging step was repeated three times and each time, the supernatant was removed, and the solvent was replaced. After the last centrifugation step, the analyte was resuspended in water. The various times of the reaction are listed in Table 1 below.

Table 1. The reactions times corresponding to each sample.

| Sample Number | Reaction Time |
|---|---|
| Sample 1 | 15 Minutes |
| Sample 2 | 30 Minutes |
| Sample 3 | 1 Hour |
| Sample 4 | 4 Hours |
| Sample 5 | 12 Hours |
| Sample 6 | 20 Hours |
| Sample 7 | 61 Hours |
| Sample 8 | 122 Hours |

Ultraviolet–visible (UV-VIS) spectroscopy was performed on these samples and a calibration curve was made via a series dilution of the stock particles. For the calibration curve, the samples were prepared in triplicates and the measurements were also triplicated. However, for the analyte, only the measurements were triplicated due to the limited supply of the samples.

Additionally, two samples of 4,4″-Bis(4,4,5,5,6,6,6-heptafluoro-1,3-dioxohexyl)-o-terphenyl-4′-sulfonyl chloride (BHHCT) metal chelates were prepared and tested. The two metals were Praseodymium (Pr) and Holmium (Ho). First, the metal oxides were dissolved in a solution of HCl which was then boiled off to obtain the metal chloride. The metal chloride was

then dissolved in a solution of ethanol where BHHCT was added for the chelation to take place. A drop cast of 10-micro liter sample of each metal chelate was analyzed.

# CHAPTER III

# RESULTS

The two approaches tested as metal tags, are MTEGME functionalized 5 nm gold nanoparticles, and BHHCT metal chelates. Both tags provide a unique detectable metal signature on mass spectra that allow for their characterization. This is essential because proteins are difficult to characterize by mass. Using SIMS for protein analysis results in fragmentation due to the nature of the instrument. When the projectile impacts the surface, it delivers an immense amount of energy to the sample. This energy allows for the ionization and desorption of secondary ions, but subsequently, it fragments large and fragile molecules such as proteins. Thus, when analyzing samples that contain large and fragile molecules, one may not observe the molecular ion, but rather fragments of the parent ion. Since proteins are composed of a limited number of amino acids varying only in their sequential arrangement, fragmentation analysis is not the optimal method of characterizing proteins.

The advantage of using tags in general, is that it allows for the bypass of direct protein characterization. One can simply analyze the tags observed in mass spectrum and infer the results to their corresponding conjugated proteins. The benefit of these tags is that they can be engineered to be sturdy to minimize fragmentation and maximize detection. This explains why metal tags are chosen to be conjugated to proteins and result in a reliable way of indirectly characterizing proteins. Aside from some metals such as iron and copper which can be seen in nature, others such as lanthanides are not observed and thus can serve as a sure way of characterizing the tag. In other words, if a rare metal such as lanthanum is used in the synthesis

of a protein tag, the emission and detection of such an element must be a result of an impact to the tag.

**MTEGME Functionalized Gold Nanoparticles**

As discussed previously, it is unlikely to see intact proteins using SIMS however, small tags can be observed entirely. Figure 4. Shows how the whole MTEGME ligand can be observed in the mass spectrum.

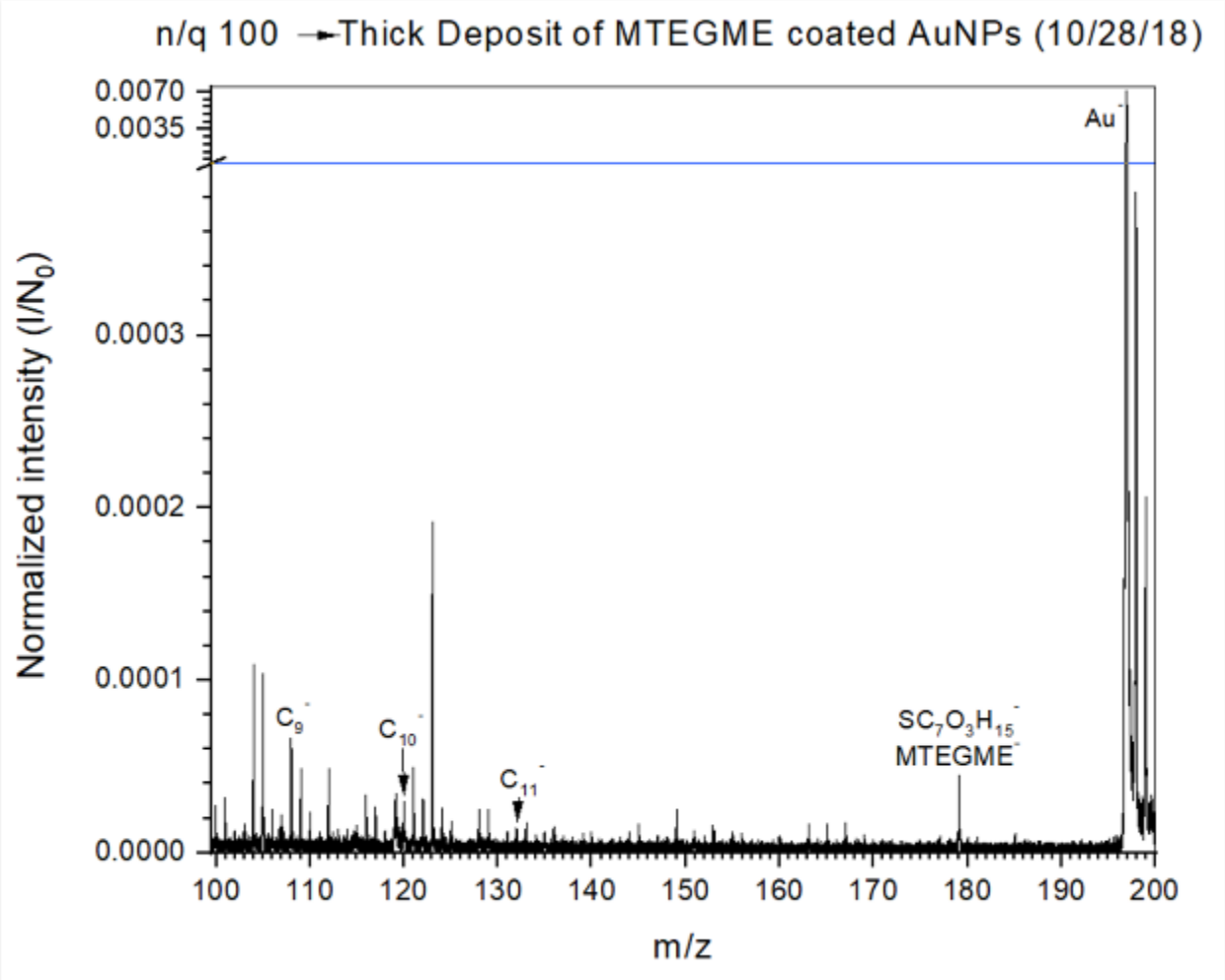


Figure 4. Mass spectrum showing MTEGME coated gold nanoparticles bombarded with 520keV, n/q 100.

Figure 4 shows a mass spectrum of normalized intensity on the Y-axis and mass to charge ratio on the X-axis. The normalized intensity is simply the total number of detected ions

divided by the total number of impacts. This mass spectrum formatting will be the same throughout all spectra displayed. At mass to charge ratio 179, the intact ligand can be observed with a single negative charge.

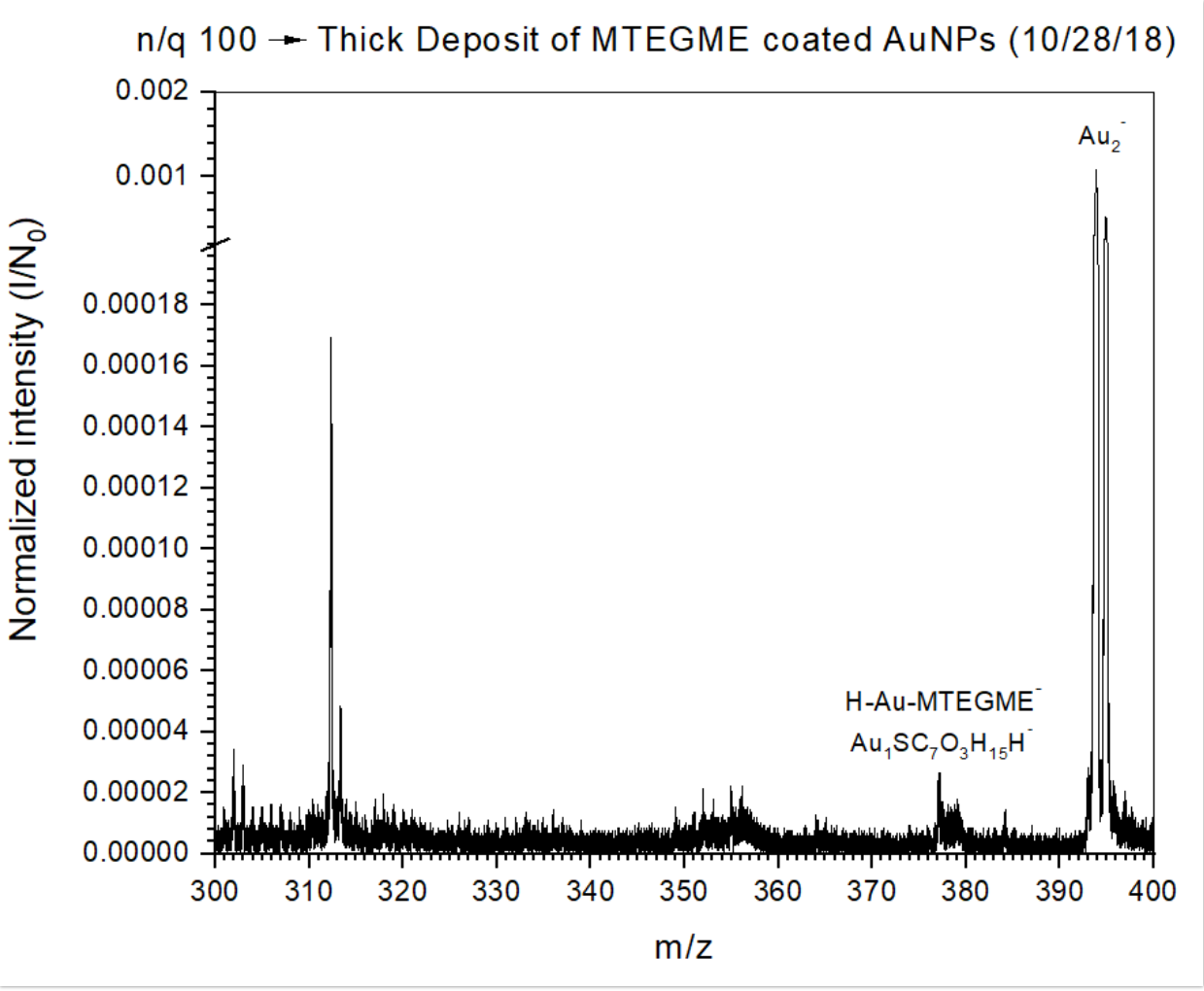


Figure 5. MTEGME ligand bound with one gold atom.

At mass to charge ratio of 377 in Figure 5, a gold atom can be observed bound to an intact ligand and a hydride. This hydride-gold-ligand complex is formed rather than simply the gold-ligand complex, because we bias negative ions. Having the gold atom bound to two separate species enables the entire complex to carry a negative charge and become detectable, rather than neutral and positive species. This hydride can be substituted with another ligand,

allowing one gold atom to bind two ligands and form a negatively charged complex as shown in figure 6.

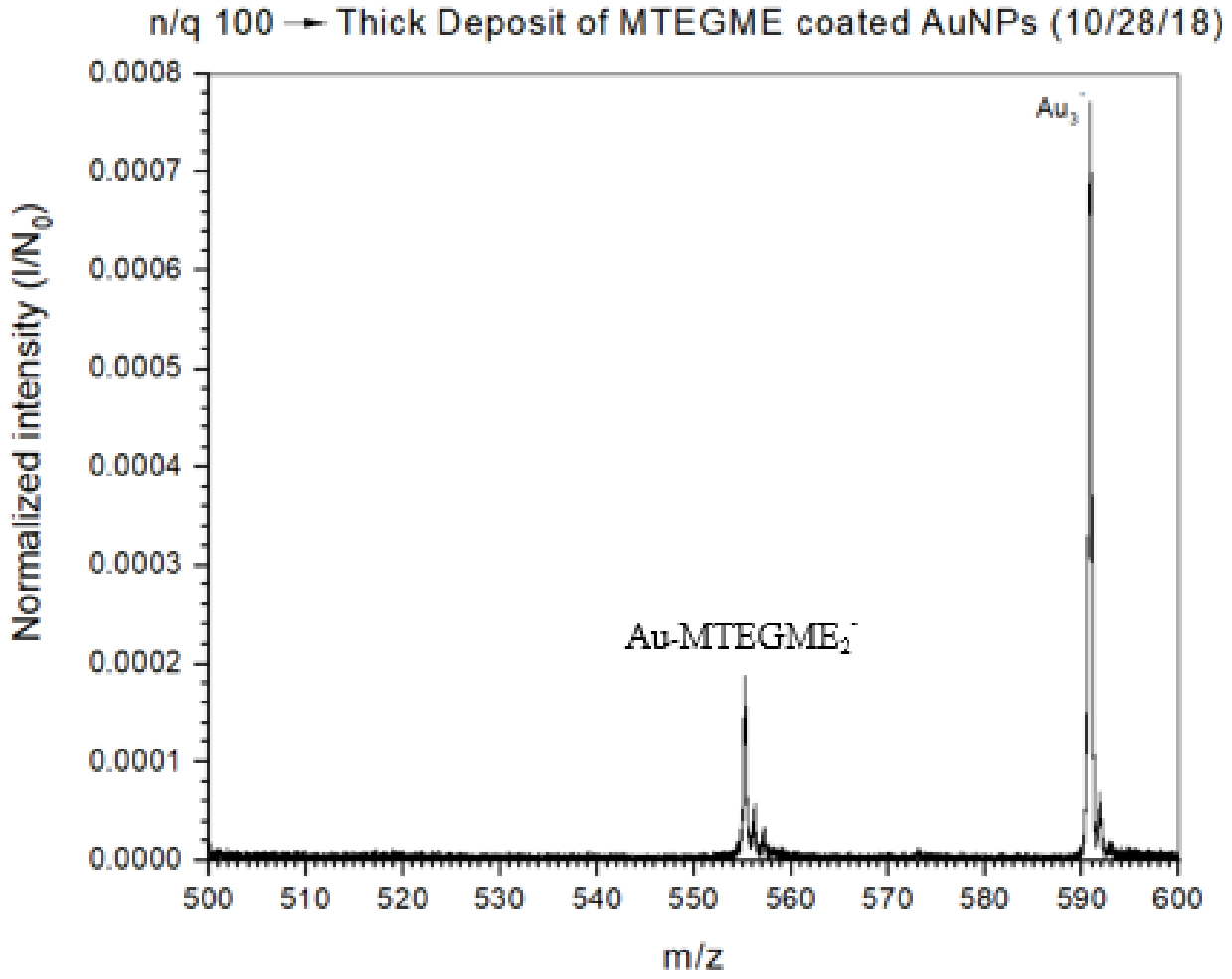


Figure 6: Gold atom bound with two intact ligands bound.

In figure 7, another relatively stable gold-ligand combination can be seen. Two gold atoms with three intact ligands bound are detected and observed.

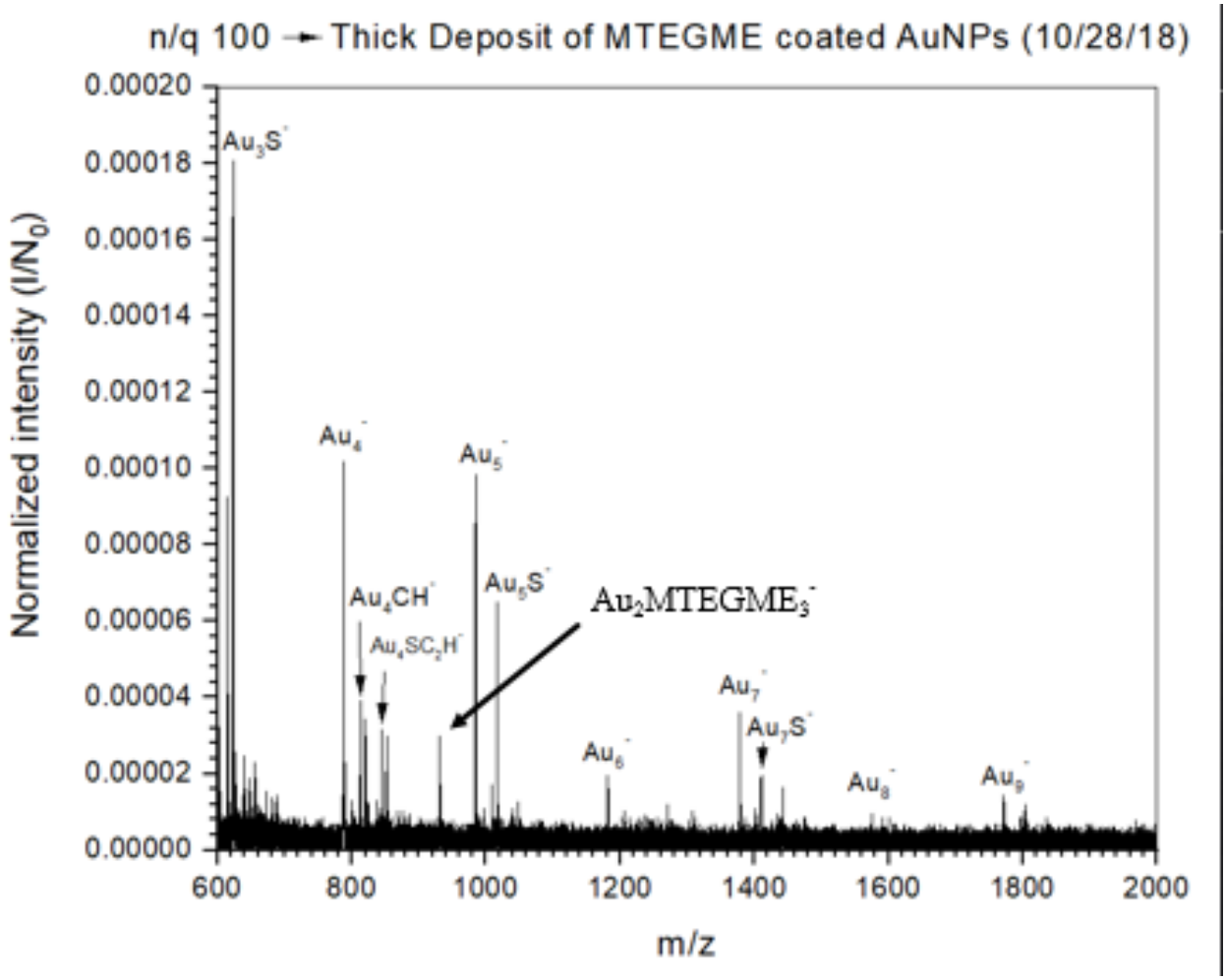


Figure 7: Two gold atoms bound with three ligands

Lastly, UV-VIS measurements were taken on the MTEGME functionalized AuNPs subjected to ligand exchange with MUA. This reaction was stopped at several time points in order to control and select for the amount of ligand exchange. In Figure 8, the absorbance of the is plotted against wavelength. All the standards that were used to make the calibration curve are plotted in black, but each sample is plotted in a different color. Sample 1 had the shortest time of reaction, while sample 8 was the longest reaction time.

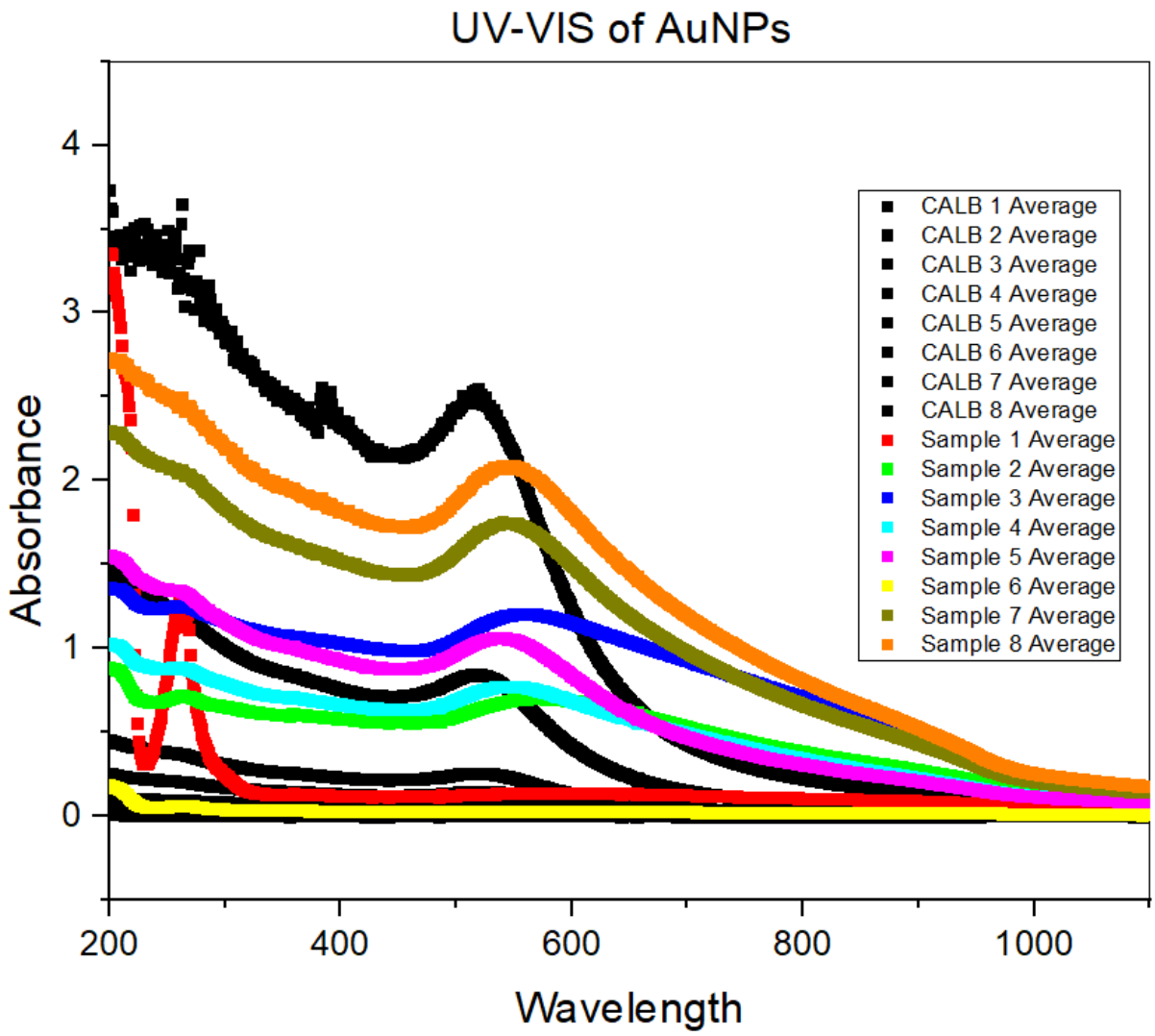


Figure 8. The absorbance vs. wavelength of all eight samples as well as the calibration standards.

Sample 1, shown above in Figure 8, had some residual ethanol in the sample, that is why it has a different pattern on the short wavelengths. When analyzing the calibration standards, there is a clear peak absorbance at wavelength of 516 nm. This peak is consistent throughout all eight calibration standards. However, when comparing this absorbance peak to the analyte samples, one could easily see a shift towards a longer wavelength. Since the shift is towards a longer wavelength, this is called a redshift. This effect is explained in detail by Barron, R., and Andrew, N., in book titled “Physical Methods in Chemistry and Nano Science”. [24] According

to the authors, the wavelength at maximum absorbance is highly depended on the environment surrounding the nanoparticles. The Mie theory is a mathematical model that can be used to describe and predict the peak absorption wavelength of nanoparticles. One variable in this model is the dielectric constant of the environment surrounding the nanoparticles. This is directly related to the surface plasmon resonance of the nanoparticles which is responsible for the absorbance of the electromagnetic radiation. If the environment surrounding the nanoparticles changes, it can cause the surface plasmon resonance to shift and absorb at a different energy, thus a different peak absorbance wavelength will be observed. This can be caused by many factors such as binding proteins or changing the ligand composition on the surface. Due to the shift observed in Figure 8, one can infer that ligand exchanged did indeed take place. This phenomenon of peak absorbance wavelength shift has been observed before, and it can even be modulated by directly controlling the functionalization of the nanostructures. [25]

Lastly, the peak absorbance values at 516 nm are plotted against the known concentrations of the prepared calibration samples in Figure 9. A linear fit was then performed to generate a trendline which could be used to calculate the nanoparticle concentration in each sample. Using beer's law, one can solve of the concentration of an analyte given the distance of light travel through the sample, the extinction coefficient, and the recorded absorbance. This will be significant in the future because the concentrations can be compared to the yield of the metal tags from the mass spectrometry analysis. However, these mass spectrometry results were not able to be obtained at the time of this reporting.

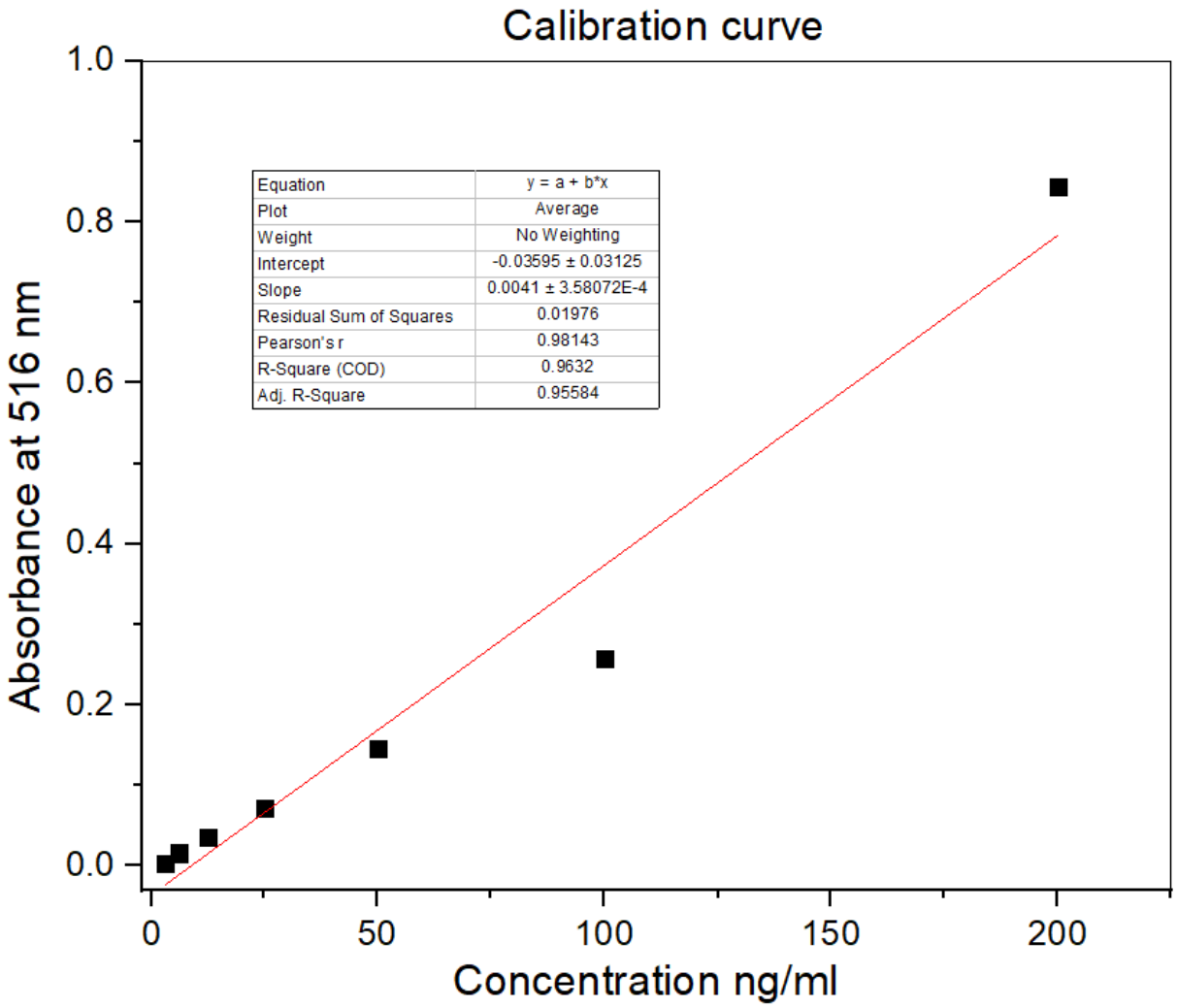


Figure 9. Calibration curve of the MTEGME functionalized AuNPs.

**BHHCT Metal Chelate**

When analyzing the BHHCT results, one must consider the structural features of the molecule. Surrounding the chelation site, there are many fluorine atoms which, although are not directly bound to the metal, are in close proximity. This explains why the mass spectrum shows many metal fluorine peaks, in Figure 10, these species are a result of a recombination that is formed upon the bombardment of the surface. Due to the amount of energy deposited on the surface by the projectile, often times the molecular ion gets fragmented and even atomized. This

results in many atoms scattering about in a cloud like plume for a brief moment, which allows the opportunity for atoms to recombine and form relatively stable species such as the metal fluoride species observed. Several combinations of metal fluoride molecules are made and can be seen in figure 10 and figure 11. These species would be unique to the metal tag in a biological sample and thus serve as a great characteristic peak that can be observed and used to characterize the tag. Since BHHCT also contains a chlorine atom, different metal chlorine/fluorine recombinations are observed.

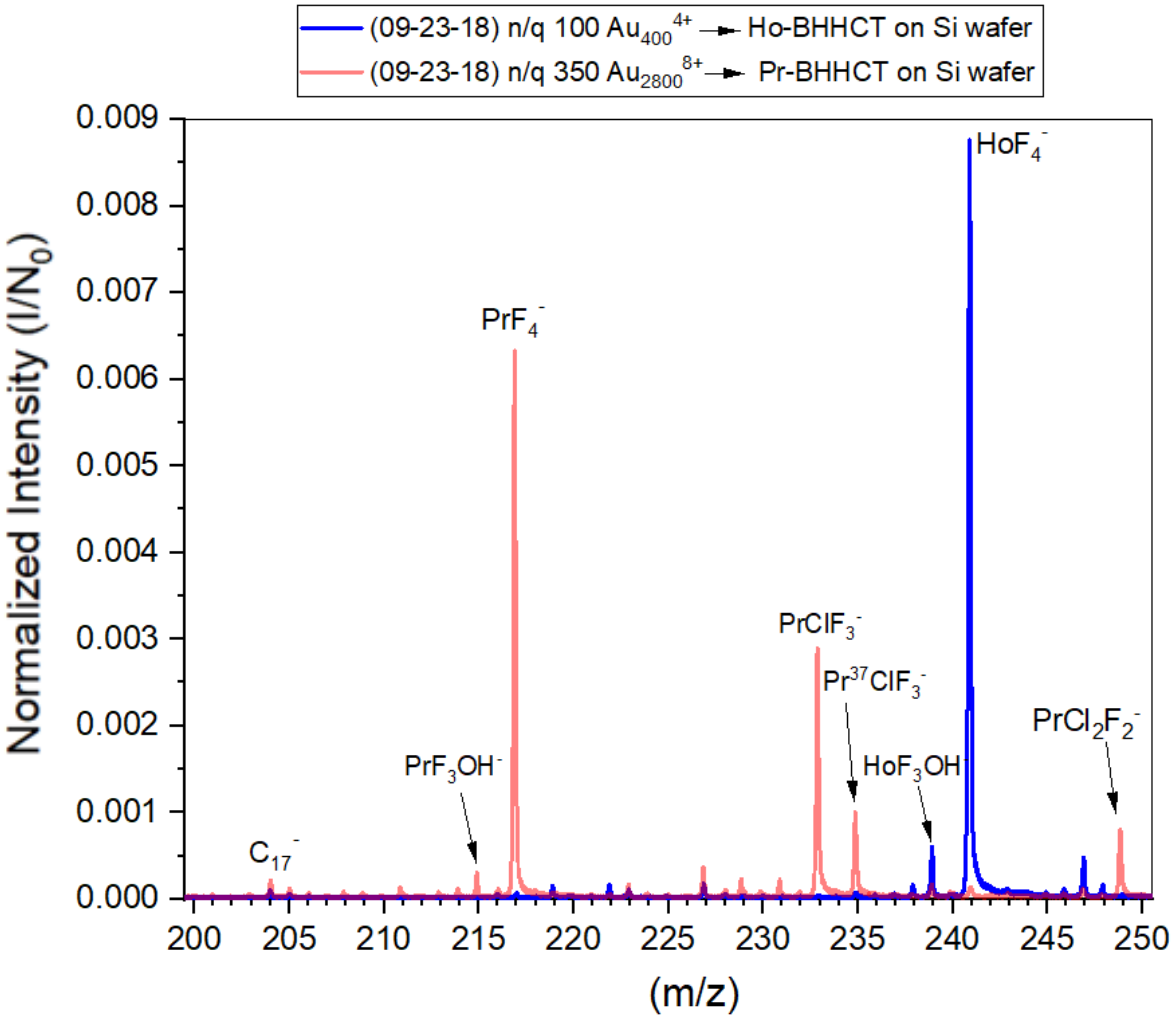


Figure 10: The metal fluoride recombinants are observed.

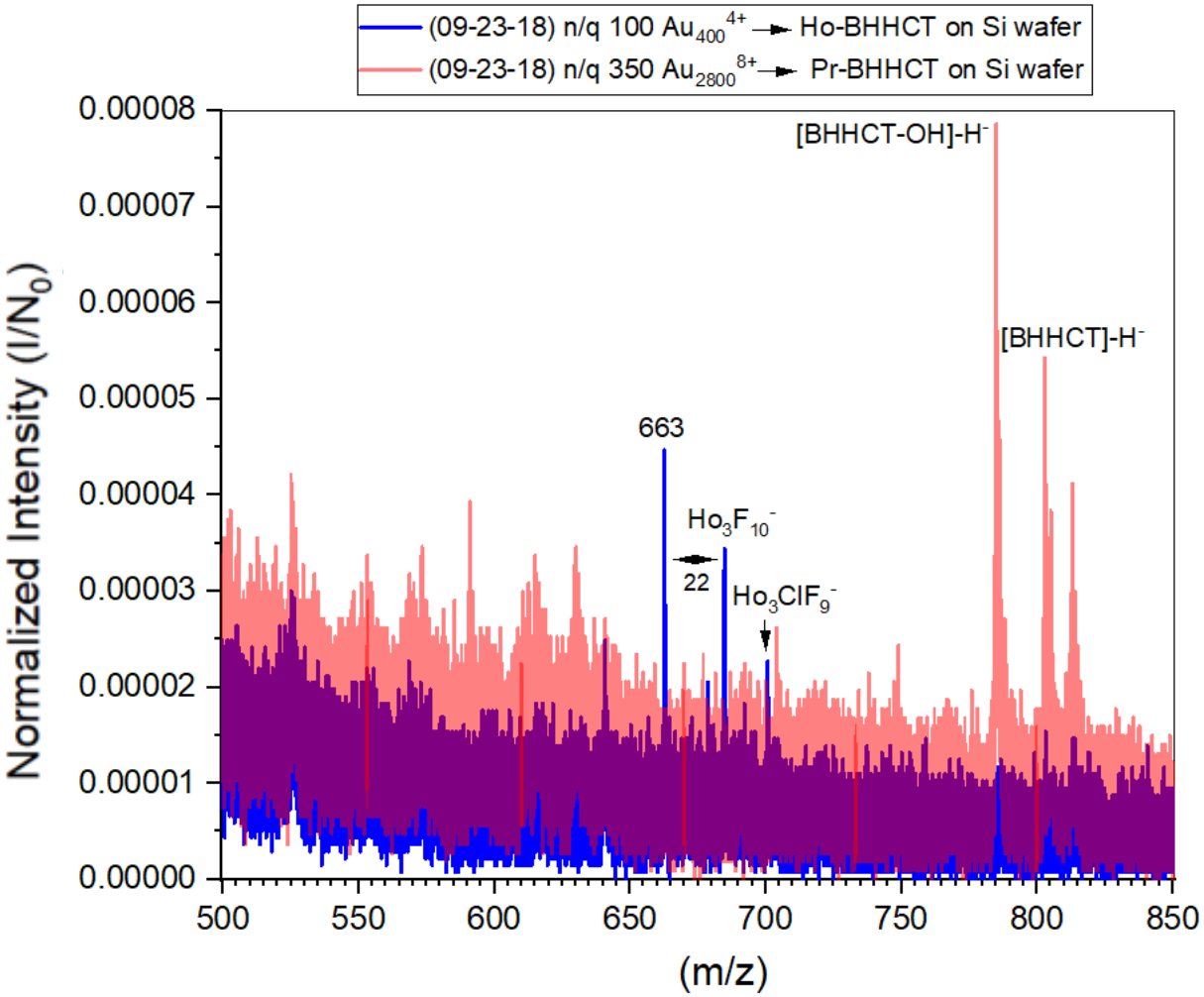


Figure 11: Intact BHHCT molecule observed in addition to Metal fluoride peaks.

In figure 11, the intact BHHCT molecule minus a hydrogen atom can be observed. It is observed as a deprotonated species because we only select for negative ions to be detected. Additionally, we observe the BHHCT molecule hydrolyzed where the terminal chlorine atom would be. This hydrolyzation can occur when moisture reaches the BHHCT solution. Lastly, two BHHCT molecules deprotonated once can be seen bound with one metal in Figure 12.

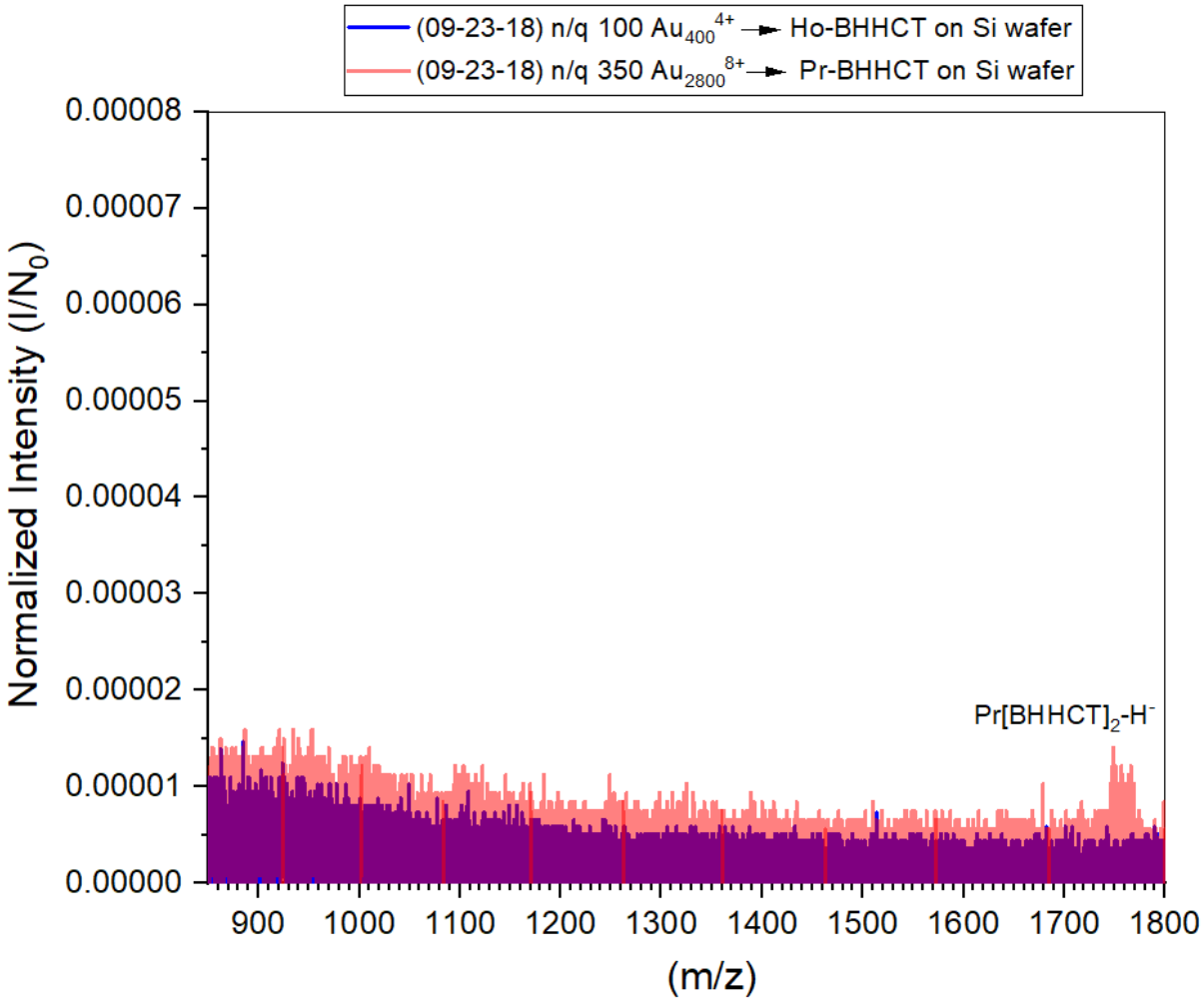


Figure 12: Two intact BHHCT molecules are observed with one metal atom.

# CHAPTER IV

# CONCLUSION

In this study, metal tags were developed in order to be applied to cluster SIMS and enable the colocalization of many proteins on the nanoscale. The two approaches that were attempted in this study were the MTEGME functionalized AuNPs, and the BHHCT metal chelate. The purpose of these tags is to enable SIMS imaging to reach into the protein analysis domain. The nanoparticles were successfully characterized using SIMS via multiple unique mass signatures. Next, it was shown how they could undergo ligand exchange which could allow for the optimization of the ligand coating, and antibody conjugation. The nanoparticles were characterized using UV-VIS spectroscopy and the peak absorbance shift was evident of the successful ligand exchange. Lastly, a calibration curve was made using a serial dilution ran in triplicate sampling and triplicate measurement to eliminate human error as well as instrumental error.

The second approach was the BHHCT metal chelate, which also showed promise in being utilized as a protein marker. The molecule is not only able to bind lanthanides, but it is also able to directly conjugate to antibodies which made it very suitable for our purpose. The two metals tested in this study were Praseodymium and Holmium, they were well characterized using SIMS. It was demonstrated how each tag was uniquely identifiable from the other and would be distinguished in a biological sample. In conclusion, this study demonstrated the potential of two metal tags in being utilized by SIMS to allow for the colocalization of proteins on the cell surface.

Lastly, recommendations for further studies with regards to the AuNPs include the conjugation of each sample, of various reaction times, to an antibody of choice. The AuNPs of each sample should have a different amount of MUA ligand bound to the surface. This will affect the extent that each nanoparticle could conjugate to the antibodies. The more MUA on the surface, the more binding sites that will be available for antibodies to attach to. Thus, future experiments should assess the extent of conjugation and the number of antibodies bound per nanoparticle. Additionally, with regards to the BHHCT metal chelate, conjugation should also be investigated and the amount of BHHCT bound per antibody should be determined and maximized. Additional metals should be chelated and characterized to build upon the library of metals that can be utilized. Then, the tags should be tested on a patterned protein surface as a proof of concept, and to demonstrate their ability of being characterized and resolved. Finally, the method should be applied and tested onto a real cell model.

# REFERENCES


1. Bendall, S.C., et al., Single-cell mass cytometry of differential immune and drug responses across a human hematopoietic continuum. Science, 2011. 332(6030): p. 687-696.

2. Bodenmiller, B., et al., Multiplexed mass cytometry profiling of cellular states perturbed by small-molecule regulators. Nature biotechnology, 2012. 30(9): p. 858-867.

3. Horowitz, A., et al., Genetic and environmental determinants of human NK cell diversity revealed by mass cytometry. Science translational medicine, 2013. 5(208): p. 208ra145-208ra145.

4. Giesen, C., et al., Highly multiplexed imaging of tumor tissues with subcellular resolution by mass cytometry. Nat Meth, 2014. 11(4): p. 417-422.

5. Bandura, D.R., et al., Mass cytometry: technique for real time single cell multitarget immunoassay based on inductively coupled plasma time-of-flight mass spectrometry. Analytical Chemistry, 2009. 81(16): p. 6813-6822.

6. Takahashi, H., et al., Imaging surface immobilization chemistry: correlation with cell patterning on non-adhesive hydrogel thin films. Advanced functional materials, 2008. 18(14): p. 2079-2088.

7. Jones, E.A., N.P. Lockyer, and J.C. Vickerman, Mass spectral analysis and imaging of tissue by ToF-SIMS—The role of buckminsterfullerene, C 60+, primary ions. International Journal of Mass Spectrometry, 2007. 260(2): p. 146-157.

8. Gamble, L.J., et al., ToF-SIMS of tissues:“Lessons learned” from mice and women. Biointerphases, 2015. 10(1): p. 019008.

9. Angelo, M., et al., Multiplexed ion beam imagining of human breast tumors. Nature Medicine, 2014. 20, 436-442

10. Steinhauser, M.L., et al., Multi-isotope imaging mass spectrometry quantifies stem cell division and metabolism. Nature, 2012. 481, 516-519.

11. Samfors, S., et al., Localised lipid accumulation detected in infarcted mouse heart tissue using ToF-SIMS. International Journal of Mass Spectrometry, 2019. 437: p. 77-86.

12. Kaya, I., et al., On-Tissue Chemical Derivatization of Catecholamines Using 4-(N-Methyl)pyridinium Boronic Acid for ToF-SIMS and LDI-ToF Mass Spectrometry Imaging. Analytical Chemistry, 2018. 90(22): p. 13580-13590.

13. Munem, M., et al., Chemical imaging of aggressive basal cell carcinoma using time-of-flight secondary ion mass spectrometry. Biointerphases, 2018. 13(3): 03B402. DOI: 10.1116/1.5016254

14. Phan, N.T., et al., MS/MS analysis and imaging of lipids across Drosophila brain using secondary ion mass spectrometry. Analytical and Bioanalytical Chemistry, 2017. 409(16): p. 3923-3932.

15. Roddy, T.P., et al., Identification of Cellular Sections with Imaging Mass Spectrometry Following Freeze Fracture. Analytical Chemistry, 2002. 74(16): p. 4020-4026.

16. Roddy, T.P., et al., Imaging of Freeze-Fractured Cells with in Situ Fluorescence and Time-of-Flight Secondary Ion Mass Spectrometry. Analytical Chemistry, 2002. 74(16): p. 4011-4019.

17. Passarelli, M.K., et al., Development of an Organic Lateral Resolution Test Device for Imaging Mass Spectrometry. Analytical Chemistry, 2014. 86(19): p. 9473-9480.

18. Tian, H., et al., Subcellular Chemical Imaging of Antibiotics in Single Bacteria Using C60-Secondary Ion Mass Spectrometry. Analytical Chemistry, 2017. 89(9), pp 5050-5057.

19. Tian, H., et al., Molecular imaging of biological tissue using gas cluster ions. Surface and Interface Analysis, 2014. 46(1): p. 115-117.

20. Tian, H., et al., Secondary-Ion Mass Spectrometry Images Cardiolipins and Phosphatidylethanolamines at the Subcellular Level. Angewandte Chemie, 2019. 131(10): p. 3188-3193.

21. Nicholas W., Imaging Mass Spectrometry on the Nanoscale with Cluster Ion Beams. Analytical Chemistry, 2015. 87(1): p. 328-333.

22. Eller, M.J., S.V. Verkhoturov, and E.A. Schweikert, Testing Molecular Homogeneity at the Nanoscale with Massive Cluster Secondary Ion Mass Spectrometry. Analytical Chemistry, 2016

23. M. J. Eller Ph.D. Dissertation, Texas A and M University 2012.

24. Pavan M. V. RajaAndrew R. Barron, Physical Methods in Chemistry and Nano Science. OpenStax CNX. Jan 17, 2019

25. Zijlstra, P., et al., Chemical Interface Damping in Single Gold Nanorods and Its Near Elimination by Tip-Specific Functionalization. Angewandte Chemie, 2012. 51(33): p. 8352-8355.